WARSAW UNIVERSITY OF TECHNOLOGY Index 351733
FACULTY OF CIVIL ENGINEERING
COMMITTEE FOR CIVIL AND WATER ENGINEERING
POLISH ACADEMY OF SCIENCES ISSN 1230-2945

DOI: 10.24425/ace.2021.138069

ARCHIVES OF CIVIL ENGINEERING

Vol. LXVII ISSUE 3 2021

s. 525–541

Research paper

Tensile validation tests with failure criteria comparison for various GFRP laminates

T. Wiczenbach[1], T. Ferenc[2]

Abstract: The paper studies the mechanical properties of glass fibre reinforced polymers (GFRP) with various types and orientation of reinforcement. Analyzed specimens manufactured in the infusion process are made of polymer vinyl ester resin reinforced with glass fibres. Several samples were examined containing different plies and various fibres orientation [0, 90] or [+45, –45]. To assess the mechanical parameters of laminates, a series of experimental tests were carried out. The samples were subjected to the uniaxial tensile tests, which allowed us to obtain substitute parameters, such as modulus of elasticity or strength. After all, results from experiments were used to validate the numerical model. A computational model was developed employing ABAQUS software using the Finite Element Method (FEM). The analysis was performed to verify and compare the results obtained from numerical calculations with the experiments. Additionally, the following failure criteria were studied, based on the index of failure I_F Maximum Stress, Maximum Strain, Tsai–Hill, and Tsai–Wu. The results confirmed the assumptions made for the footbridge's design purpose, which is made using examined material. Moreover, comparing the experimental and numerical results found that in the linear-elastic range of the material, they are consistent, and there is no significant difference in results.

Keywords: Composite structure, Failure criteria, GFRP laminate, Unidirectional test, Validation

[1] M.Sc.Eng., Gdańsk University of Technology, Faculty of Civil and Environmental Engineering, Gabriela Narutowicza 11/12, 80-233 Gdańsk, e-mail: tomasz.wiczenbach@pg.edu.pl, ORCID: https://orcid.org/0000-0001-8482-0580

[2] PhD., Eng., Gdańsk University of Technology, Faculty of Civil and Environmental Engineering, Gabriela Narutowicza 11/12, 80-233 Gdańsk, e-mail: tomasz.ferenc@pg.edu.pl, ORCID: https://orcid.org/0000-0002-2551-7570

1. Introduction

The new requirements for materials concerning mechanical and physical properties better than those traditionally used, i.e., steel, ceramics, reinforced concrete, led to creating a group of materials referred to as composite materials. Composite materials are produced to diminish the mass of structures or engineering structures, as they have a better strength-to-weight ratio. Commonly, they are used in the aircraft, car, and shipbuilding industry, and they become more prevalent in civil engineering [6, 11, 15, 20, 22], especially in bridge structures [3, 18, 23].

Nevertheless, their anisotropic characteristics make them crucial to understand and determine their attitude under dynamic or static loads [12, 14, 16]. Due to the growth of their use, the determination of these materials' mechanical properties has become the main topic [2, 7, 10, 24, 25]. Laminates, which constitute a group of structural composites, are defined by specific physical and mechanical properties. In practice, assessing all physical and mechanical parameters of these materials is very costly and time-consuming. However, a group of features called basic physical properties has been developed [12, 16]. This class of properties can be determined with relatively simple methods. However, they provide crucial information about the material being tested. The most relevant example is studying the properties of the materials under tension, or more precisely, the features that can be calculated from the curve obtained in the uniaxial off-axis tensile test [25]. This test involves deforming a specimen with specified dimensions at a constant velocity and measurement of force.

Conducting the experiments is a capable approach for researching the mechanical properties of composite materials. Nonetheless, it is often costly and requests a large number of resources [5]. One of the main features in designing composite materials is to diminish these experimental costs, but at the same time, achieve overall examination results. Consequently, numerical simulations using the finite element method (FEM) are being conducted to model the behavior of structures made of laminate. Pierluigi et al. [4] developed a behaviour of steel beams reinforcement by pultruded CFRP strips. The proposed laminate model implemented a connection between the beam and adhesive nodes to achieve whole structure deformation. Hussein et al. [8] modelled a non-linear analysis of concrete samples covered with an FRP jacket. The laminates were modelled with the use of shell elements. Ferenc et al. [9] investigated a sandwich structure made of GFRP laminate skin and foam core. The whole structure was modelled using ESL theory with the use of shell elements. In this way, the numerical results are compared to the experimental test results, allowing validating numerical models. The extended studies could be taken with a properly developed numerical model.

Due to composite materials' complicated structure, such structures' modeling is often based on experimental tests result. Furthermore, in practical design, a more sophisticated analysis must be considered. Several theories can be applied to the numerical design of composite materials, especially laminates. Composite can be modelled through Equivalent Single Layer (ESL) theory, two-dimensional continuum – Layer-wise theory (LW), or three-dimensional continuum [1, 17, 19]. According to the ESL theory, the laminate is treated as a shell with only one ply with equivalent substitute parameters. The LW theory takes into account each ply of laminate but still considers it as shells. The 3D idea is the most accurate and complex, but on the other hand, the most complicated and time-consuming. The choice of an appropriate approach depends on the desired accuracy of the results and the system's geometry. The equation can calculate the total number of nodes: for 3D $n\cdot(m+1)$, LW $n\cdot m$, and ESL theory is n, where n is a number of nodes on one surface, and m is a number of layers. According to Fig. 1, there are $11^2=121$ nodes in ESL theory (Fig. 1a), $11^2\cdot 3=363$ nodes in LW (Fig. 1b), and $11^2\cdot(3+1)=484$ nodes in 3D theory (Fig. 1c). Conclusively, by using ESL theory, the number of degrees of freedom is reduced. Since the research presented in this article is related to the footbridge, which works as a shell and sandwich structure, the tested laminate will work mainly in two directions. On the scale of the footbridge, the thickness of the laminate is negligible. Therefore the ESL theory was analyzed, in which the third dimension (thickness) is reduced, leaving a two-dimensional shell.

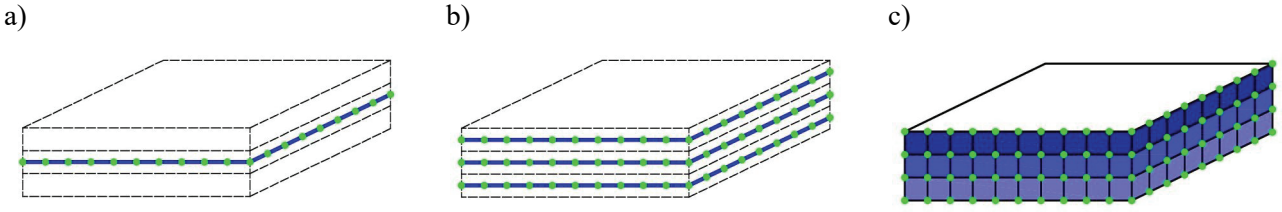

Fig. 1. Model: a) ESL theory, b) LW theory, c) 3D theory

Therefore, the paper introduces an experimental and numerical study of how laminates' components impact their mechanical parameters. The numerical model was developed to perform the examination efficiently by verifying the linear results with the experimental tests through ABAQUS that use the FEM. The effects of the number of plies and their direction were investigated. Moreover, the study found a specific range of justified use of linear-elastic theory in GFRP laminate modelling. The results supply beneficial information to establish the usefulness design of a structure made of GFRP laminates. Moreover, the footbridge design's assumptions, in which GFRP laminate material is used, were confirmed.

2. Materials and methods

2.1. Examined material

The subject of the study is a GFRP laminate made of the following components: flame retardant vinyl ester resin Firestop S 440 as a matrix (produced by BUFA Gelcoat Plus, Germany), and E (electric) glass stitched fabrics BAT800 or GBX800 as a reinforcement (produced by DIPEX, Slovakia). Each fabric consists of two layers of reinforcement with an equal amount of fibres in two directions 400 g/m^2 orientated: [0/90] for BAT (Fig. 2a) and [+45/–45] for GBX (Fig. 2b).

a) b)

Fig. 2. Fiber orientation for: a) BAT, b) GBX

Each lamina was analyzed as a homogenous orthotropic material. Its elastic and strength parameters were determined in the laboratory of the Military University of Technology [13] in series of tests conducted on a new post-cured material according to proper standards: unidirectional in-plane tension according to ISO 527-1 [25], unidirectional in-plane compression according to ISO 14126, in-plane shear according to ISO 14129, out-of-plane shear according to ISO 14130 and non-standardized out-of-plane compression test. The material parameters were determined in temperature $T = 20°C$ in the principal material directions, denoted as the lamina plane. The samples were lying in the environment, which had a temperature 23 ±2°C and relative humidity $50 \pm 10\%$ for more than 88 hours. The tests were performed under the same conditions. The average values of the material constants, based on five specimens in each trial, are collected in Table 1. Standard deviations did not exceed 5% the average values.

Seven types of laminates were studied: denoted from P1 to P7, each contains a various number of plies and its reinforcement. The single-ply has thickness 0.663 mm and is reinforced with fabric, either BAT or GBX. The stack sequence of all investigated laminates is listed in Table 2.

Table 1. Material Properties of the GFRP for single-ply [13]

Parameter		Description	Value	Unit
E_1	E_2	longitudinal (1) and transverse (2) elastic moduli	23.4	GPa
ν_{12}		Poisson's ratio	0.153	–
G_{12}		in-plane shear modulus	3.52	GPa
G_{13}	G_{23}	transverse shear moduli	1.36	GPa
$R_{1,t}$	$R_{2,t}$	longitudinal (1) and transverse (2) strength in tension	449	MPa
$R_{1,c}$	$R_{2,c}$	longitudinal (1) and transverse (2) strength in compression	336	MPa
R_{12}		in-plane shear strength	45.2	MPa
R_{13}	R_{23}	transverse shear strength	34.7	MPa
$\varepsilon_{1,t}$	$\varepsilon_{2,t}$	longitudinal (1) and transverse (2) failure strain in tension	0.0291	–
$\varepsilon_{1,c}$	$\varepsilon_{2,c}$	longitudinal (1) and transverse (2) failure strain in compression	0.0148	–
γ_{13}	γ_{23}	transverse shear failure strain	0.0356	–

Table 2. The sequence of plies in all specimens

Specimen	Stack sequence of plies	Fiber angles	Type of sample
P1	[BAT,GBX,GBX,BAT] = [BAT,GBX$_2$,BAT]	[0/90], [+45/–45]	III
P2	[BAT,BAT,BAT,BAT] = [BAT$_4$]	[0/90]	I
P3	[BAT,BAT,BAT,BAT,BAT,BAT] = [BAT$_6$]	[0/90]	I
P4	[BAT,BAT,BAT,BAT,BAT,BAT,BAT,BAT] = [BAT$_8$]	[0/90]	I
P5	[GBX,GBX,GBX,GBX] = [GBX$_4$]	[+45/–45]	II
P6	[GBX,GBX,GBX,GBX,GBX,GBX] = [GBX$_6$]	[+45/–45]	II
P7	[GBX,GBX,GBX,GBX,GBX,GBX,GBX,GBX] = [GBX$_8$]	[+45/–45]	II

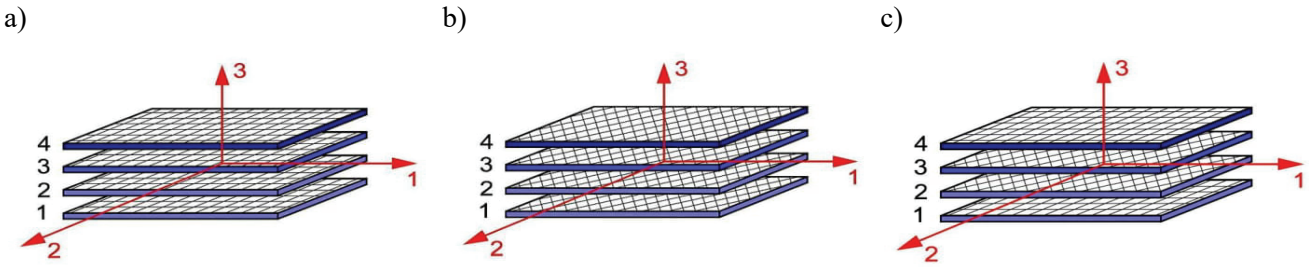

Fig. 3. Example sequence of the plies in specimen: a) [BAT$_4$], b) [GBX$_4$], c) [BAT,GBX$_2$,BAT]

The tests' main aim was to verify whether the number of layers and the reinforcement orientation impact the mechanical properties of the GFRP laminates. Therefore, three different samples were investigated: type I, II, III, listed in Table 2. An example of the arrangement of layers in a tested laminate is presented in Fig. 3. The first type of sample consists of two-way reinforcement parallel (BAT) to the first global direction, as shown in Fig. 3a, while the second type of specimens has reinforcement at an angle of 45 degrees (GBX) to the first global direction (Fig. 3b). The third type of samples contains both types of reinforcement (BAT and GBX) mentioned in the two previous types (Fig. 3c).

2.2. Tests specimens and test stand

The dimensions of investigated specimens (Fig. 4) were assumed according to ISO 527-4 standard, which specifies the test condition to determine tensile properties of orthotropic FRP composite. The total length was 250 mm, the width 25 mm, while the thickness was varied and depended on specimens and is presented in Table 3:

Table 3. The number of plies and thickness of specimens

Specimen	Number of layers	Thickness [mm]
P1, P2, P5	4	2.79
P3, P6	6	4.02
P4, P7	8	5.17

The grip separation was 150 mm, while the gauge length for an extensometer was about 50 mm longitudinally (Fig. 5a). The specimens were prepared by water-cutting out of the plates after the post-curing process. Each of the seven plates was manufactured in the same conditions in the infusion process.

The uniaxial tensile test procedure for plastics is specified in the following standards: ISO 527-1 [26], which defines the general principles for conducting experiments. ISO 527-4 standard contains a description of properties for the tension of isotropic and orthotropic reinforced plastics. Examined material is anisotropic, but for simplicity, the laminates' properties were determined by standard ISO 527-4. This standard specifies the shape of samples and the method of determining the individual characteristic.

The study focused on the extension of GFRP specimens and comparing the mechanical properties related to the extension. The samples were to be used in a composite sandwich bridge, in which the skins work mainly in the state of elongation or compression.

The uniaxial tensile tests were conducted on a computer-operated Zwick/Roell type machine. The machine (Fig. 5b) consists of two grips, one of which is fixed, and the second is movable with constant force or displacement. The initial force was assumed at the level of 200 N. The experiments were carried out at a constant traverse speed of 2 mm/minute to reach the sample’s destructive force. The displacement of grips, as well as applied load, were recorded. Additionally, the extensometer was used to measure displacements (strains) in the middle of the investigated specimen length.

a) b)

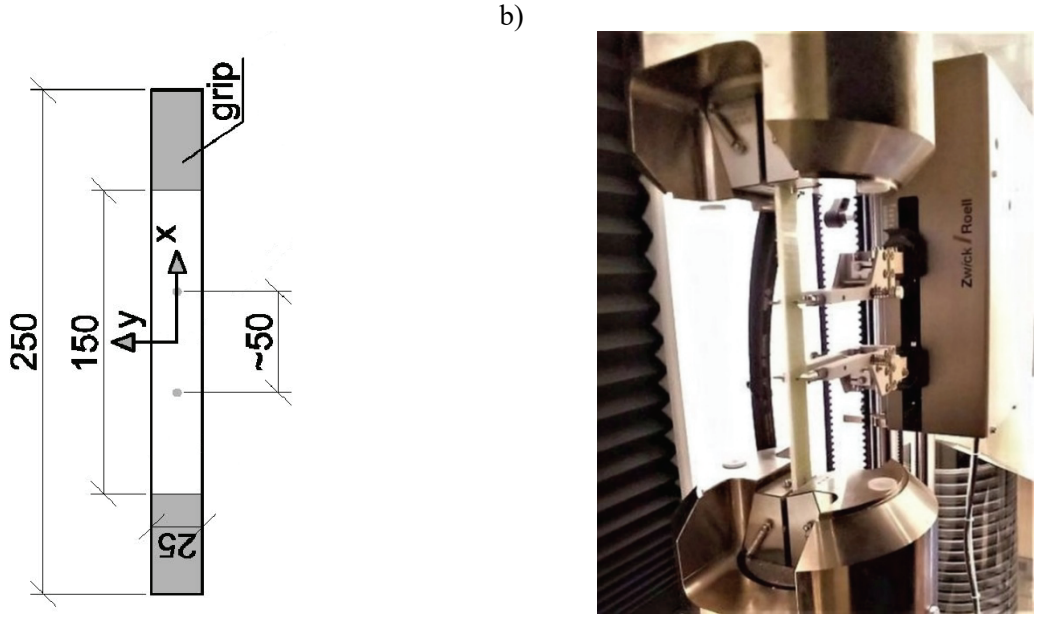

Fig. 5. a) Dimensions of unidirectional specimen [mm], b) The test stand for the uniaxial tensile test

3. Experimental results

Seven different GFRP laminates (from P1 to P7) were investigated. Five uniaxial tensile tests were conducted for each specimen. Results were presented as the curve of stress-strain relation in Fig. 6. due to the testing machine's capacity, the destructive force of the specimen P4 (Fig. 6c) could not be obtained. Additionally, all samples (excluding P4) cracked suddenly upon reaching failure strength and was damaged between the grips.

Modulus of elasticity can be determined, according to standard ISO 527-1, as (3.1):

$$E_{ISO} \equiv E_x = \frac{\sigma_2 - \sigma_1}{\varepsilon_2 - \varepsilon_1} \tag{3.1}$$

where:

σ_2 – longitudinal stress obtained, when longitudinal strains $\varepsilon_2 = 0.0025$, σ_1 – longitudinal stress obtained, when $\varepsilon_2 = 0.0005$.

The first range of strain was taken after standard ISO 527-1:1993 and was $[0.0005; 0.0025]$, which is represented in Fig. 6 with vertical green lines. The second range was chosen individually $[0.01; 0.02]$ and is presented with vertical red lines. The arithmetical average values of moduli of

elasticity for two ranges are listed in Table 4. Additionally, average destructive force, average maximum stress, and average maximum strain at failure are given. The presented results show that number of plies do not influence the mechanical properties of GFRP laminates.

However, as can be observed in stress-strain curves (Fig. 6), laminates' stiffness decreases after strain reaches a specific value. For type I, this value is $\varepsilon = 0.004 - 0.005$. Hence, after this point, the stress-strain relation is different. This phenomena sometimes referred to as the "knee effect", occurs because the matrix's capacity is being exceeded, and microcracks occur [21]. Nevertheless, despite decreased stiffness, the laminate can still carry the load, and maximum force is up to five times higher.

What is more, this phenomena can also be observed in Fig. 6g for type III. Besides, the graphs of first type specimens show bilinear character. Moreover, the second type also shows the linear curve in the initial stage. Subsequently, after a specific point curve becomes non-linear and plastic strains distinctly increase. Such results can not be called the "knee effect", but the shear of the matrix. The III type of samples exhibits the state of the first and second types, which can be seen in the graph Fig. 6g. "Knee effect" can be only observed in the type of specimens, which contains BAT reinforcement. Therefore, in further analyzes, the corresponding values were used as for P1-P4 samples, i.e. $\varepsilon = 0.004 - 0.005$.

Table 4. Obtained values from the experimental analysis for all specimens

Specimen	$E_{x,1}$ GPa	$E_{x,2}$ GPa	Avg. F kN	Avg. σ MPa	Avg. ε –
P1	18.4	11.1	17.88	265.82	0.0218
P2	23.3	14.9	30.69	435.09	0.0271
P3	23.3	15.2	47	469.15	0.0294
P4	23.3	15.1	–	–	–
P5	13.7	1.7	8.75	135.22	0.0630
P6	13.6	2.8	16.94	179.53	0.0874
P7	13.7	2.4	20.19	165.31	0.0819

That is why for each sample, two values of moduli of elasticity are determined. Due to the bilinear character of the obtained curves, especially for type I and III, the modulus of elasticity was determined in two strain ranges by linear approximation (linear regression) using the Least Squares Method. In this method, the result is approximated to a linear function in the form of $y = \alpha x + \beta + e,$ where e is the error between the value of the measured and approximating function. The method involves estimating the parameters α and β so that the function, according to the formula, obtains the smallest value.

(3.2) $$S_r = \sum_{i=1}^{n} e_i^2 = \sum_{i=1}^{n} (y_i - \alpha x_i - \beta)^2$$

I type

II type

a)

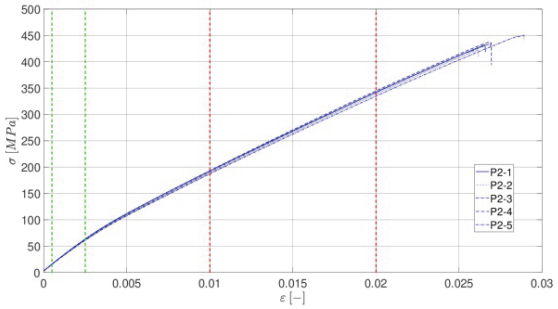

d)

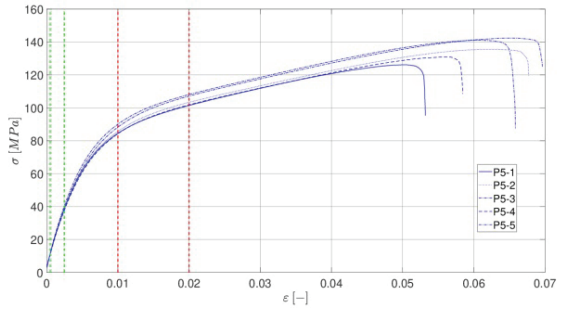

b)

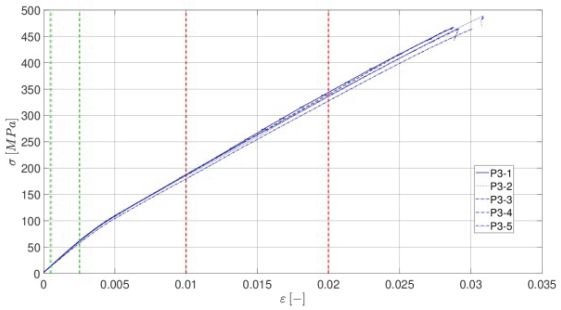

e)

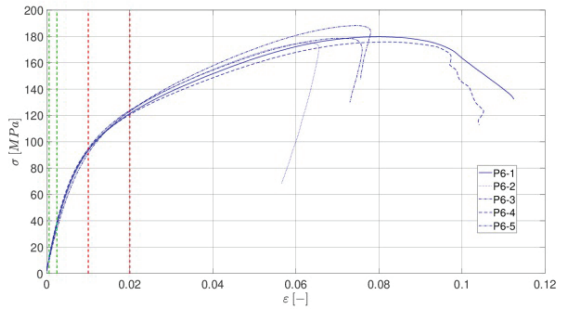

c)

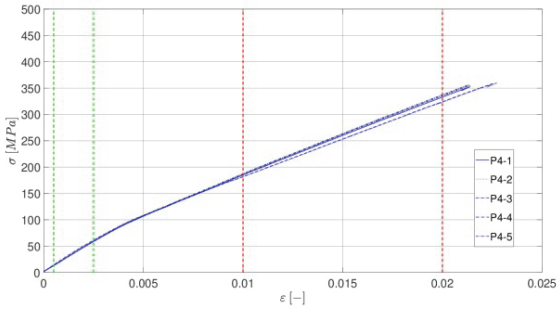

f)

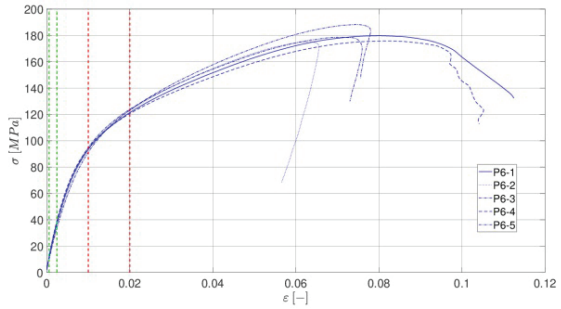

III Type

g)

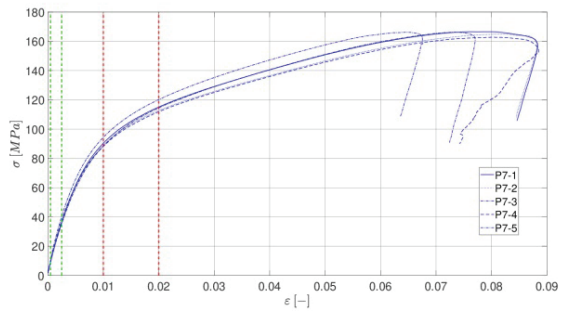

Fig. 6 The longitudinal strain-stress curve for specimens: a) P2, b) P3, c) P4, d) P5, e) P6, f) P7, g) P1

4. Numerical results

The numerical simulations of the GFRP laminates were conducted through the FEM in commercial software Abaqus. To obtain mechanical parameters, i.e., moduli of Young, numerical calculations of specimens P1 to P7 were performed.

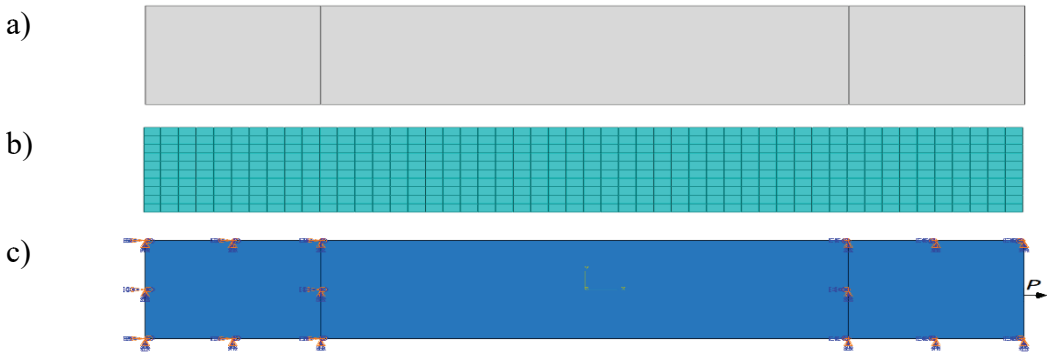

Fig. 6 a) Visualization of the model, b) Meshgrid, c) Boundary conditions and applied force

The model was built by four-node shells with linear shape functions and full integration. The GFRP laminates were modelled as a multi-layer shell, using the ESL theory (Fig. 6a), to simulate this type of material's homogeneous characteristics. An element with dimensions of 5×5 mm was adopted, which gives a total number of 300 finite elements and 366 nodes (Fig. 6b). The grips of the tensile machine were not modelled themselves. Instead, it was assumed that one area (25×50 mm) is fixed, the other area (25×50 mm) is movable in the longitudinal direction just like it is in the testing machine. A point load was applied, as shown in Fig. 6c. The calculations were conducted to the maximum load value of 20000 N. This value of force was chosen according to the experimental failure results. The analysis was carried out with the assumption of the material's linear elasticity and assuming small displacements by the first-order theory.

The results of numerical analysis allowed us to add the new stress-strain relations to experimental results. The use of an extensometer on the same samples permitted a direct comparison of the obtained results. That confirmed the accuracy of the results obtained from numerical simulations comparing to experiments. The experimental test allowed to determine the substitute global properties of the samples. The numerical model's validation was for the needs of the footbridge design [20]. In the actual structure, the laminate should not exceed the specified value of stresses. This value corresponds to a specific value of strains, which identified with the “knee effect”. After this point, it could cause further degradation of the material. As a consequence, calculations were performed in the linear (“design”) range only.

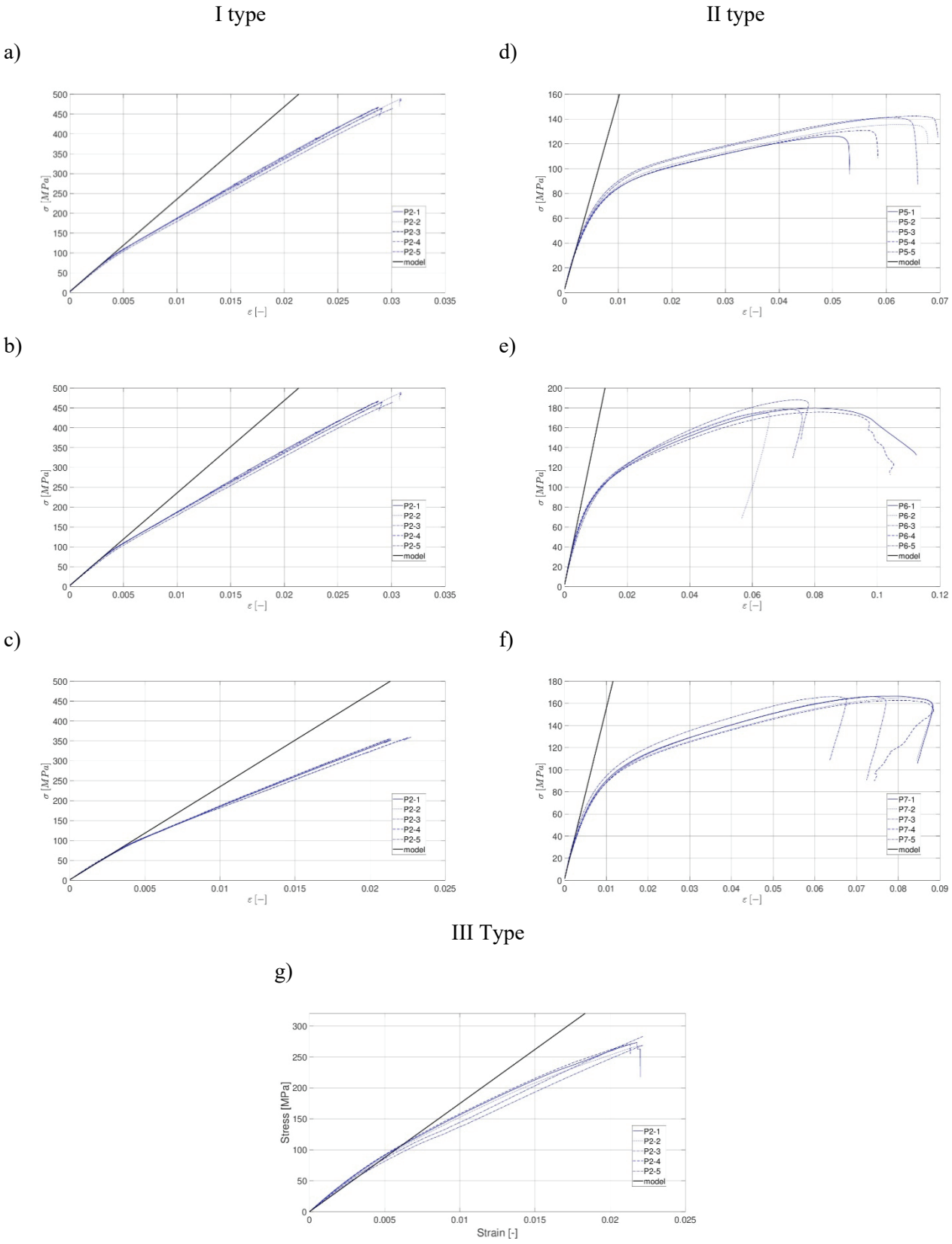

Fig. 7 The longitudinal strain-stress curve for specimens: a) P2, b) P3, c) P4, d) P5, e) P6, f) P7, g) P1

The numerical analysis results were plotted and compared with the experimental part's values in Fig. 7a–g with a continuous black line. As it is presented, the simulations are accurate until reaching the specific value of longitudinal strain. After this value, the stiffness of the material decrease due to matrix capacity is extended.

Moreover, a comparison of substitute values of moduli of elasticity obtained from the numerical analysis was compared with those obtained from experiments. The values measured in tensile tests, which are listed in Table 5, are presented only for the first range of strain, according to ISO 527-1. In this range, the accuracy is very high, and the approximation error is below 1%. The results presented in this table are vital to validate the linear elastic part of the numerical models.

Table 5. Comparison of Young's Modulus values from the experimental and numerical analysis

Sample	P1	P2	P3	P4	P5	P6	P7
Exp. [GPa]	18.4	23.3	23.3	23.3	13.7	13.6	13.7
Mod. [GPa]	18.3	23.4	23.4	23.4	13.6	13.6	13.6
Error [%]	0.5	0.6	0.5	0.6	0.9	0.1	0.6

5. Comparison of failure criteria

The assessment of the strength of laminate, which can be expressed as the extreme external load applied on it, is, on the one hand, very relevant for a designer of structure, but on the other, very difficult. Due to the orthotropic behavior of laminates, some classic criteria may not be applied. However, the paper consist of a comparison of the primary strength criteria, sometimes called biaxial criteria, the criterion of maximum strain, the criterion of maximum stress, the criterion of Tsai-Hill, and the criterion of Tsai-Wu.

All mentioned above criteria not considering any damage mechanisms inside the composite [16]. The observation level used by them is the ply globally treated as homogenous material, not its components and their various possible failure mode like in Hashin criteria.

Failure criteria were calculated for studied specimens P1 to P7 employing Abaqus software. The stress-based failure theories characterize a surface surrounding the origin in the three-dimensional space, similarly to strain-based theory. Failure appears any time a state of stress or strain is on or outside this surface. From the calculations, the failure index IF is obtained. Calculations were made for force 40000 N. Physical meaning of the chosen value of force is that the experimental samples failures at this point.

Table 6. Obtained values for failure criteria and the experimental

Specimen		P1		P2	P3	P4	P5	P6	P7
		BAT	GBX	BAT	BAT	BAT	GBX	GBX	GBX
Experiment	ε [–]	0.0218		0.0271	0.0294	–	0.063	0.0874	0.0819
	σ [MPa]	265.82		435.09	469.15	–	135.22	179.53	165.31
Max. Strain	ε [–]	0.0291	0.014514	0.0305	0.0305	0.0305	0.02664	0.02664	0.02664
	δ [%]	33.49	33.42	12.55	3.74	–	57.71	69.52	67.47
Max. Stress	σ [MPa]	448.999	102.621	449.001	448.999	448.999	148.571	148.571	148.571
	δ [%]	68.91	61.39	3.19	4.29	–	9.81	17.24	10.13
Tsai-Hill	σ [MPa]	372.57	100.603	389.668	389.673	389.675	145.43	145.431	145.431
	δ [%]	40.16	62.15	10.44	16.94	–	7.55	18.99	12.05
Tsai-Wu	σ [MPa]	381.316	99.548	426.816	426.818	426.819	148.281	148.281	148.281
	δ [%]	43.45	62.55	1.91	9.03	–	9.66	17.41	10.03

It was concluded that the results obtained experimentally do coincide with numerical results, excluding the maximum strain theory. A comparison of the experimental failure stress/strain and numerical failure criteria are listed in Table 6. Additionality, the absolute approximation error was calculated to compare the results. Calculated approximation error δ relates to comparing experimental results (v_{approx}) and numerical failure analysis (v) values.

$$\delta = \left|\frac{v - v_{approx}}{\mathrm{v}}\right| \cdot 100\% \tag{5.1}$$

For Maximum Strain theory, the experiment's average failure strain deviates from those obtained according to the criterion. The Maximum Strain criterion is used to predict the failure of unidirectional fiber–reinforced composites. This criterion argues that strain in the principal directions of material decided about the efforts of material. Differences are mostly because the tested material is bidirectionally reinforced. The stress-based theories describe more precisely the failure of the specimens and are more consistent with experimental results. Nevertheless, the criterion of maximum stress is very similar to the previous one. In this model, the stress level in the principal directions of material decides if damage occurs. More complex criteria used to determine the failure of the laminates are expressed by the second-order function, which is the sum of the ratios of the state of stress related to the mechanical parameters of the laminate. Tsai-Hill criterion assumes that tensile and compressive strength are identical in composite material's main orthotropic axes. Tested material has different values of strength in tension and compression. The Tsai-Wu criterion is used to assess composites' failure in multi-axial stress states in the form of so-called tensors of strength. The most precise results are obtained by the Maximum Stress and Tsai-Wu

criterion. The first one provides a failure of the sample only in the principal directions of material. The tested specimens were subjected only to one-directional stress.

For this reason, the result of this criterion is close to the experimental results. The results converge with the longitudinal in the first global direction and transverse in the second global direction strength in tension (Table 1). On the other hand, Tsai-Wu defines the samples' failure in multi-axial stress states, to which real constructions are subjected. Summarizing the Tsai-Wu failure criterion's characteristics, the most similar results to the experimental one were obtained.

Additionally, due to the presented results, the Tsai-Wu criterion was chosen to implement a composite structure design. Hence, calculations according to this criterion were conducted to obtain the failure index when the "knee effect" occurs. This kind of micro-damage cannot be allowed for design purposes. Therefore, it is important to estimate the value of the failure index IF correctly. Despite the laminate's relatively high strength, this value cannot be exceeded in the structure under load. The computation was performed only to the specific value of strain $\varepsilon = 0.004$. The failure index IF, which were computed for specific value of strain, for specimens P1 is IF = 0.2494 for BAT layer and IF = 0.5763 for GBX layer, P2–P4 is IF = 0.2086 and P5-P7 is IF = 0.4999. Thus, for design purposes, IF according to the Tsai-Wu criterion was assumed at this level. Furthermore, this factor cannot be exceeded in any ply of laminate. On this basis, it was assumed in the design process, the failure index IF = 0.2.

6. Conclusion

This paper presents research on the influence of fiber layers number and orientation on mechanical properties for seven different GFRP specimens. However, the results obtained in the experimental and numerical analysis are convergent and mechanical parameters do not depend on the number of layers. However, results vary for different orientations of layers (BAT and GBX). The failure criteria used in the analysis do not depend on the number of layers.

What is more, the orthotropic material that was used in the research has different mechanical properties in different directions. It could be observed that mechanical properties vary for different fiber angles. Fig. 8 presents the effect of reinforcement orientation on the mechanical properties, i.e., Young's modulus, obtained numerically. The numerical analysis was performed only on one layer with different fiber orientations. Additionally, with red squares are shown the values obtained experimentally (for Type I and II). For a bidirectionally reinforced material, the same values for

corresponding angles f.e. 0° and 90° degrees, 15° and 75° degrees, 30° and 60° degrees are achieved. Moreover, for the fibers at 45° degrees, the stiffness modulus's lowest value is obtained.

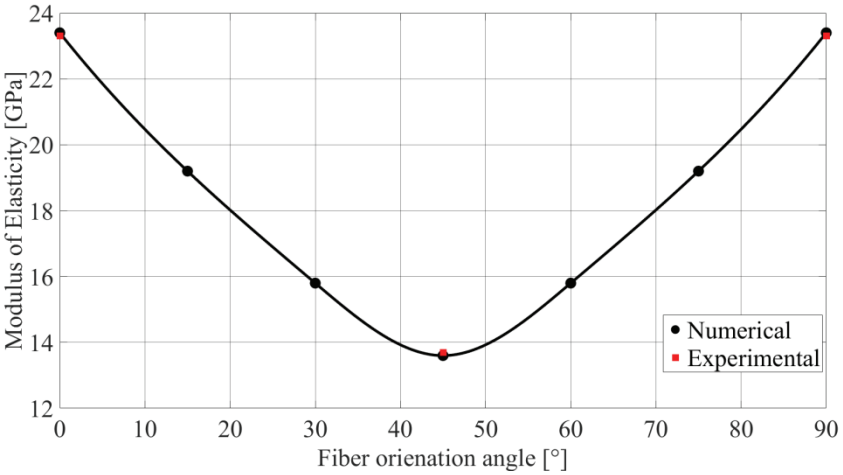

Fig. 8. Young's modulus as a function of fiber orientation

The experimental examination revealed that for a specific value of longitudinal strain, which is $\varepsilon = 0.004–0.005$ for type I and type III, a decrease in the material's stiffness occurs due to extended matrix capacity. This phenomenon can be referred to as the "knee effect". It could be observed plastic strains for specimens P5–P7 (type II), and the samples were shear deformed.

Performed computations have shown that the compatibility of calculations can be obtained by substituting multilayered laminates with a single-layered shell using ESL theory. Moreover, numerical calculations were performed only in a linear, where, by definition, the material is supposed to work only in the linear range, and therefore "knee effect" can not occur. Comparing the results, it was found that in the linear-elastic range of the material, the results are consistent, and there is no significant difference in results, which confirms assumptions made for laminate modelling.

Additionally, a few various failure criteria were tested. The results from strain-based theory are not convergent with results received experimentally. However, the stress-based theories are more precisely accurate with experimental results. The most convergent results were obtained for the Tsai-Wu theory. Finally, for the Tsai-Wu criterion, the indices of failure were computed for the specific value of strain when the "knee effect" occurs. For design purposes of composite structures, the failure index, according to the Tsai-Wu criterion, cannot exceed IF = 0.20.

References

[1] H. Altenbach, J. Altenbach, and W. Kissing, *Mechanics of Composite Structural Elements*. Berlin, Heidelberg: Springer Berlin Heidelberg, 2004.

[2] E. Barbero, J. Fernández-Sáez, and C. Navarro, "Statistical analysis of the mechanical properties of composite materials," *Composites Part B: Engineering*, vol. 31, no. 5, pp. 375–381, Jul. 2000. https://doi.org/10.1016/S1359-8368(00)00027-5

[3] J. Chróścielewski, T. Ferenc, T. Mikulski, M. Miśkiewicz, and Ł. Pyrzowski, "Numerical modeling and experimental validation of full-scale segment to support design of novel GFRP footbridge," *Composite Structures*, vol. 213, pp. 299–307, Apr. 2019. https://doi.org/10.1016/j.compstruct.2019.01.089

[4] P. Colombi and C. Poggi, "An experimental, analytical and numerical study of the static behavior of steel beams reinforced by pultruded CFRP strips," *Composites Part B: Engineering*, vol. 37, no. 1, pp. 64–73, Jan. 2006. https://doi.org/.1016/j.compositesb.2005.03.002

[5] S. C. M. D'Aguiar and E. Parente Junior, "Local buckling and post-critical behavior of thin-walled composite channel section columns," *Latin American Journal of Solids and Structures*, vol. 15, no. 7, Jul. 2018. https://doi.org/10.1590/1679-78254884

[6] I. Danilov, "Some Aspects of CFRP Steel Structures Reinforcement in Civil Engineering," *Procedia Engineering*, vol. 153, pp. 124–130, 2016. https://doi.org/10.1016/j.proeng.2016.08.091

[7] J. Di, L. Cao, and J. Han, "Experimental Study on the Shear Behavior of GFRP–Concrete Composite Beam Connections," *Materials*, vol. 13, no. 5, p. 1067, Feb. 2020. https://doi.org/10.3390/ma13051067

[8] H. M. Elsanadedy, Y. A. Al-Salloum, S. H. Alsayed, and R. A. Iqbal, "Experimental and numerical investigation of size effects in FRP-wrapped concrete columns," *Construction and Building Materials*, vol. 29, pp. 56–72, Apr. 2012. https://doi.org/10.1016/j.conbuildmat.2011.10.025

[9] T. Ferenc, Ł. Pyrzowski, J. Chróścielewski, and T. Mikulski, "Sensitivity analysis in design process of sandwich U-shaped composite footbridge," in *Shell Structures: Theory and Applications Volume 4*, CRC Press, pp. 413–416, 2017. https://doi.org/10.1201/9781315166605-94

[10] R. Haj-Ali and H. Kilic, "Non-linear behavior of pultruded FRP composites," *Composites Part B: Engineering*, vol. 33, no. 3, pp. 173–191, Apr. 2002. https://doi.org/10.1016/S1359-8368(02)00011-2

[11] M. Heshmati, R. Haghani, and M. Al-Emrani, "Environmental durability of adhesively bonded FRP/steel joints in civil engineering applications: State of the art," *Composites Part B: Engineering*, vol. 81, pp. 259–275, Nov. 2015. https://doi.org/10.1016/j.compositesb.2015.07.014

[12] K. Kaw, *Mechanics of Composite Materials*. CRC Press, 2005.

[13] M. Klasztorny, D. B. Nycz, R. K. Romanowski, P. Gotowicki, A. Kiczko, and D. Rudnik, "Effects of Operating Temperatures and Accelerated Environmental Ageing on the Mechanical Properties of a Glass-Vinylester Composite," *Mechanics of Composite Materials*, vol. 53, no. 3, pp. 335–350, Jul. 2017. https://doi.org/10.1007/s11029-017-9665-9

[14] I. Kreja, "A literature review on computational models for laminated composite and sandwich panels," *Open Engineering*, vol. 1, no. 1, Jan. 2011. https://doi.org/10.2478/s13531-011-0005-x

[15] S. Moy, "Advanced fiber-reinforced polymer (FRP) composites for civil engineering applications," in *Developments in Fiber-Reinforced Polymer (FRP) Composites for Civil Engineering*, Elsevier, pp. 177–204, 2013. https://doi.org/10.1533/9780857098955.2.177

[16] J. N. Reddy, "Theory and Analysis of Laminated Composite Plates," in *Mechanics of Composite Materials and Structures*, Dordrecht: Springer Netherlands, pp. 1–79, 1999.

[17] J. N. Reddy, "A Simple Higher-Order Theory for Laminated Composite Plates," *Journal of Applied Mechanics*, vol. 51, no. 4, pp. 745–752, Dec. 1984. https://doi.org/10.1115/1.3167719

[18] M. Rostami, K. Sennah, and S. Hedjazi, "GFRP Bars Anchorage Resistance in a GFRP-Reinforced Concrete Bridge Barrier," *Materials*, vol. 12, no. 15, p. 2485, Aug. 2019. https://doi.org/10.3390/ma12152485

[19] A. Sabik and I. Kreja, "Linear analysis of laminated multilayered plates with the application of zig-zag function," *Archives of Civil and Mechanical Engineering*, vol. 8, no. 4, pp. 61–72, Jan. 2008. https://doi.org/10.1016/S1644-9665(12)60122-8

[20] P. P. Sankholkar, C. P. Pantelides, and T. A. Hales, "Confinement Model for Concrete Columns Reinforced with GFRP Spirals," *Journal of Composites for Construction*, vol. 22, no. 3, p. 04018007, Jun. 2018. https://doi.org/10.1061/(ASCE)CC.1943-5614.0000843

[21] Wen and S. Yazdani, "Anisotropic damage model for woven fabric composites during tension–tension fatigue," *Composite Structures*, vol. 82, no. 1, pp. 127–131, Jan. 2008. https://doi.org/10.1016/j.compstruct.2007.01.003

[22] H. Xin, Y. Liu, A. S. Mosallam, J. He, and A. Du, "Evaluation on material behaviors of pultruded glass fiber reinforced polymer (GFRP) laminates," *Composite Structures*, vol. 182, pp. 283–300, Dec. 2017. https://doi.org/10.1016/j.compstruct.2017.09.006

[23] H. Xin, A. Mosallam, Y. Liu, C. Wang, and Y. Zhang, "Analytical and experimental evaluation of flexural behavior of FRP pultruded composite profiles for bridge deck structural design," *Construction and Building Materials*, vol. 150, pp. 123–149, Sep. 2017. https://doi.org/10.1016/j.conbuildmat.2017.05.212
[24] J. E. Yetman, A. J. Sobey, J. I. R. Blake, and R. A. Shenoi, "Mechanical and fracture properties of glass vinylester interfaces," *Composites Part B: Engineering*, vol. 130, pp. 38–45, Dec. 2017. https://doi.org/10.1016/j.compositesb.2017.07.011
[25] S. Zhang, C. Caprani, and A. Heidarpour, "Influence of fibre orientation on pultruded GFRP material properties," *Composite Structures*, vol. 204, pp. 368–377, Nov. 2018. https://doi.org/10.1016/j.compstruct.2018.07.104
[26] Determination of tensile properties of plastics. Part 1: General principles, Geneva, Switzerland, 1993.

Walidacja testów rozciągania z porównaniem kryteriów zniszczenia dla różnych laminatów GFRP

Słowa kluczowe: materiały kompozytowe, kryterium zniszczenia, laminat GFRP, statyczna próba rozciągania, walidacja

Streszczenie:

W artykule zbadano właściwości mechaniczne polimerów wzmocnionych włóknem szklanym (GFRP) o różnych typach i orientacji zbrojenia. Analizowane próbki, wytworzone w procesie infuzji, wykonane są z polimerowej żywicy winyloestrowej wzmocnionej włóknem szklanym. Zbadano kilka próbek zawierających różną liczbę warstw, a także różną orientację włókien [0/90] lub [+45/–45]. Aby ocenić parametry mechaniczne laminatów, przeprowadzono szereg badań eksperymentalnych. Próbki poddano testom jednoosiowego rozciągania, co pozwoliło uzyskać parametry zastępcze, takie jak moduł sprężystości czy wytrzymałość. Wyniki eksperymentów posłużyły do walidacji modelu numerycznego. Model obliczeniowy opracowano za pomocą oprogramowania ABAQUS z wykorzystaniem metody elementów skończonych (MES). Analizę przeprowadzono w celu zweryfikowania i porównania wyników otrzymanych z obliczeń numerycznych z wynikami eksperymentów. Dodatkowo zbadano następujące kryteria zniszczenia, w oparciu o wskaźnik zniszczenia IF: Maksymalne naprężenie, Maksymalne odkształcenie, Tsai-Hill i Tsai-Wu. Wyniki potwierdziły założenia przyjęte przy projektowaniu kładki, którą wykonano z badanego materiału. Ponadto porównując wyniki eksperymentalne i numeryczne stwierdzono, że w zakresie liniowo-sprężystym materiału są one spójne i nie ma istotnych różnic w wynikach.

Received: 2021-01-12, Revised: 2021-02-26